CONF-820896--5

DE83 007861

NUCLEAR SHAPE TRANSITIONS AND SOME PROPERTIES OF ALIGNED-PARTICLE CONFIGURATIONS AT HIGH SPIN

T. L. Khoo, P. Chowdhury, H. Emling[a], D. Frekers,

R. V. F. Janssens and W. Kühn

Argonne National Laboratory*, Argonne, IL 60439 USA

A. Pakkanen[b], Y. H. Chung, P. J. Daly, Z. W. Grabowski

H. Helppi[b] and M. Kortelahti

Purdue University, W. Lafayette, IN 47907 USA

S. Bjørnholm, J. Borggreen, J. Pederson and G. Sletten

Niels Bohr Institute, Risø, Denmark

Abstract

Two topics will be addressed in this paper. First, we discuss the variation of shapes with spin and neutron number for nuclei in the N ≈ 88 transitional region. Second, we present comments on the feeding times of very high spin single-particle yrast states.

*This research was partially supported by the U. S. Department of Energy under Contract W-31-109-Eng-38.

[a] Visitor from GSI, Darmstadt, W. Germany.

[b] Present address: Dept. of Physics, University of Jyväskyla, Jyväskyla, Finland.

I. Shape Transition in the N=88 Region

Nuclei with N=82-86 are spherical in the ground state, but become oblate at high spin along the yrast line as successive high-j nucleons align their spins along the symmetry axis. On the other hand, nuclei with N > 90 are prolate up to the highest observed spins. One illustration of this point is the absence of nanosecond isomers of high multiplicity in nuclei with N > 90 [1]. It appears that the shell effects which drive nuclei prolate are not overcome at high spin.

The transitional nuclei with N ~ 88 lie between the above two classes of nuclei and may exhibit aspects of both classes. In fact, Bengtsson et al. [2] have pointed out that while the low-lying yrast states of the N=88 nuclei are of transitional character, a prolate deformation sets in for I > 6. We might wonder if a further change to oblate shapes occurs at higher spins, as suggested by liquid drop considerations [3]. The transitional nuclei provide a testing ground for studying the interplay of oblate-driving and prolate-driving effects, and also the variation of nuclear structure with spin and neutron number within one common framework. This last point may be understood by examining the Hamiltonian [Ref. 2].

$$H = H_o - \varepsilon\hat{Q} - \Delta(\hat{P} + \hat{P}^{+}) - \omega\hat{I}_x - \lambda\hat{N}$$

The Lagrange multipliers ω (rotational frequency) and λ (Fermi energy) have been introduced to constrain the spin and neutron number: $I = \langle\hat{I}x\rangle$ and $N = \langle\hat{N}\rangle$. Thus it may be seen that I and N can be treated on an equal footing with respect to their influence on nuclear structure.

The different modes of generating angular momentum as a function of spin and neutron number are illustrated in Fig. 1. For N = 82-86, the yrast angular momentum arises mainly from the alignment of the spins of a few nucleons around the symmetry axis. The large concentration of orbits around the equator and the subsequent core polarization lead to an overall oblate shape of $\beta \sim 0.1\text{-}0.2$. For the well-deformed prolate nuclei with $N \gtrsim 98$, the yrast states are usually generated by the familiar collective rotation around an axis perpendicular to the symmetry axis. In nuclei between these two regions both single-particle and collective modes contribute at high spin, as the spins of high-j nucleons align along the rotation axis in response to the Coriolis force, giving rise to backbending.

We had previously systematically delineated the structure of Dy isotopes with N = 82-86 [Ref. 4] while the spectroscopy of the isotopes with N > 90 is well known from other studies. Thus, to examine the transitional N=88 region, we chose to concentrate on ^{154}Dy. We performed γ spectroscopic measurements using the ^{124}Sn (^{34}S,4n) reaction, with 145-165 MeV ^{34}S beams from the Argonne superconducting linac. A comprehensive set of experiments was undertaken, including measurements of γ-γ coincidences with 3 Ge(Li) detectors, angular distributions, excitation functions and lifetimes with electronic and recoil distance techniques. In all experiments ^{154}Dy transitions were enhanced by requiring coincidences with the sectors of a large NaI crystal operated either as a sum spectrometer or as a multiplicity filter.

The level scheme of ^{154}Dy in Fig. 2 [Ref. 5] shows for $I < 32$ features similar to those of the neighboring heavier nuclei which have

intermediate prolate deformation. The positive parity yrast levels are connected by a sequence of stretched E2 transitions with energies which increase smoothly except around two backbends at I=14 and 30. This is also seen on a plot of I_x vs $\hbar\omega$ (Fig. 3), where $I_x = \{(I + 1/2)^2 - K^2\}^{1/2}$ and $\hbar\omega = \frac{E(I+2) - E(I)}{2}$. The ground band shows a rapidly increasing moment of inertia, $\mathcal{J}^{(1)} = \frac{I_x}{\omega}$, symptomatic of a transitional nucleus. On the other hand, the S-band - which is probably the rotation-aligned $i_{13/2}$ band - seemingly shows a stable character, as revealed by the fact that its points lie along a straight line nearly going through the origin. This implies almost constant values of $\mathcal{J}^{(1)}$ and $\mathcal{J}^{(2)}$, where $\mathcal{J}^{(2)} = \frac{dI_x}{d\omega}$. The reason for this behavior of the S-band is difficult to understand, particularly in view of the discussion which presently follows.

Near the highest spins the uninterrupted cascade of stretched E2 transitions - which provides a good signature of collectivity - gives way to predominantly dipole transitions of 1035 and 878 keV. Furthermore, above I=30 there is a fragmentation of the γ-flow which is quite different from those observed in backbending nuclei. Finally, the combined state lifetimes and feeding times of the highest levels at 10976 and 12297 keV, 6±1 and 5±1 ps respectively, are significantly longer than the values of $\lesssim$ 0.5 ps observed in the more collective cases such as ^{156,158}Dy (Ref. 6 and 7). All these features point towards a change from collective to single-particle nature at the highest spins observed in ^{154}Dy. The single-particle configurations are likely to be similar to the aligned-particle states of the adjacent nucleus ^{152}Dy. In this mass region, where the Fermi level is located near the beginning of the high-j orbits, only such single-particle configurations would be

expected to become yrast. As in the lighter Dy isotopes an oblate mass distribution is expected to be associated with these states. Thus, ^{154}Dy probably represents the first example of a shape transition from prolate to oblate in a heavy nucleus.

The results of the lifetime measurement are summarized in Fig. 4, which shows the spin-dependence of the quantity Q_o(eff), defined as $[\frac{16\pi}{5} B(E2; I \to I-2)]^{1/2} / \langle I\ 2\ 0\ 0 \mid I-2\ 0\rangle$. This is the usual intrinsic quadrupole moment for a K=0 band of an axially symmetric rotor. The values of Q_o(eff) reflects sizeable collectivity already at low spins, increasing between spins 2 and 6 to a value near those of the more well-formed nuclei. However, at higher spins (I = 22-32) there is a decrease in collectivity, presaging the eventual onset of single-particle transition rates for I > 33.

In the high spin limit, a rigidly rotating triaxial body has $Q_o(\text{eff}) \propto \beta \cos(30° - \gamma)$, where β and γ are the usual parameters characterizing quadrupole deformation and axial asymmetry [8]. Since the shape is prolate ($\gamma = 0°$) for $I \lesssim 14$ and likely oblate ($\gamma = -60°$) for I > 33, it is reasonable to suppose that the decrease in Q_o(eff) arises to a significant extent from a change in γ, as schematically indicated in Fig. 5. [Values of β and γ cannot be separately extracted from a measurement of only Q_o(eff)]. Thus it is probable that the transition from oblate to prolate occurs via triaxial shapes.

It has earlier been pointed out by Emling et al. [Ref. 6] that there is reduction in Q_o(eff) associated with rotation alignment in ^{156,158}Dy. They have also suggested that this could be due to the onset of triaxiality. In comparing the even Dy isotopes with A=154-158, it is seen that the reduction is more pronounced the smaller the mass.

Indeed it is only in ^{154}Dy that the transition to the single-particle limit has been attained.

This limit is reached at I=33, shortly after the second backbend at I=30. The available body of data thus suggests that rotation alignment is influential in the shape change. The first backbend is probably due to the alignment of a pair of $i_{13/2}$ neutrons. It is not clear which orbits are responsible for the second backbend in ^{154}Dy since either a second $i_{13/2}$-neutron pair or a $h_{11/2}$-proton pair [9] are expected to align around a frequency of $\hbar\omega \sim 0.4$ MeV. In fact it is possible that by this frequency all 6 orbits referred to above are rotation-aligned and that it is this action which precipitates the occurrence of the oblate shape.

In Fig. 6 we sketch how rotation-alignment may influence the shape. When the spin of a high-j particle aligns along the rotation vector, the orbit acquires an oblate mass distribution with respect to this axis. The degree to which this orbit polarizes the core determines the axial asymmetry. The soft core of a transitional nucleus (such as ^{154}Dy), in which the prolate-driving forces are just emerging, is thus susceptible to a shape change upon the rotation-alignment of several pairs of nucleons.

At the lowest spins all the angular momentum arises from collective rotation perpendicular to the symmetry axis. However, as pairs of nucleons successively align along the perpendicular axis, the spin carried by the aligned particles grows until it constitutes the total angular momentum in the oblate limit.

An interesting way of viewing this point is illustrated in Fig. 7, which was stimulated by the comparison with the behavior of neutron

stars. The gradual decrease in the rotational frequency of the surface of such stars is interrupted by sharp increases which occur about every 2 y (Fig. 7a). In Fig. 7b is shown the frequency of the rotating nuclear core as a function of the time following the $^{124}Sn(^{34}S,4n)$ ^{154}Dy reaction at 155 MeV. (For purposes of preparing this figure we assume a small intensity in the cascade proceeding through the 9351 keV level.) The corresponding spin of the aligned particles is shown in Fig. 7c. Sudden changes of alignment at the backbends give rise to fluctuations in the core frequency. (The fractional frequency change in the nuclear case is much larger than that for the neutron star-quakes!) The separation into collective and single-particle components of spin is probably not as distinct as has been assumed here, particularly as the oblate limit is approached. Nevertheless, this example serves to illustrate the increasing role of the single-particle mode at the highest spins (i.e., earliest times).

We conclude this section by reviewing the status of the shapes of Dy isotopes as a function of spin and neutron number in Fig. 8, using a plot first introduced by Bengtsson et al. [2]. Near the boundary between the regions of oblate aligned-particle configurations and of prolate rotors at $N \sim 88$, both modes of excitation appear along the yrast line. The rotation-aligned S-bands form an intermediate region in the transition between these modes both as a function of I and N. The theoretical predictions [2,10] are also indicated in Fig. 8, and are seen to be in qualitative agreement with the experimental observations.

II. Some Properties of High Spin Aligned-particle Configurations

The highest spin recorded for a discrete state is 40--in ^{152}Dy. It is an experimental challenge to detect yrast states at even higher spin and there are also important theoretical questions associated with such a pursuit. For instance, are the highest angular momenta generated by single-particle or collective modes? In cases such as ^{152}Dy, where the yrast configurations are of aligned-particle character up to the highest known spins, when and how quickly do the collective excitations set in? What are the feeding pathways for the very highest spin states? Since the preceding cascades of the highest spin states have limited multiplicity--of the order of 10--we may gain more direct insight than has previously been possible into the continuum cascades and thereby into the states excited above the yrast line. Valuable information, for instance, may be derived from knowledge of the feeding times.

A Niels Bohr Institute-Argonne-Purdue collaboration is currently performing a series of experiments on ^{147}Gd and preliminary results are reported here. This nucleus presents a favorable case for high-spin yrast spectroscopy. The occurrence of a 550 ns isomer ($I^{\pi} = 49/2^{+}$ [Ref. 11] or 47/2 [Ref. 12]) provides a clean tag for the transitions feeding the isomer. Furthermore the known [4] states above the isomer can be strongly populated in the (^{30}Si,4n) reaction.

The experimental arrangement we have used consisted of 4 Ge detectors and 16 NaI crystals, including sections of a sum spectrometer. A pulsed beam with 0.5 μs on- and 1.5 μs off- durations was employed. In-beam events in the Ge detectors were accepted only if they were accompanied by (i) a prompt cascade in the NaI array of multiplicity > 2 and (ii) at least one delayed NaI event in the beam-

off period. Ge-Ge coincidences were recorded with a DC beam, and with similar requirements as above for prompt and delayed events in the NaI array.

The preliminary level scheme above the 550 ns isomer is shown in Fig. 9. The spin assignments are from Refs. [4] and [11]. There are no spin assignments for the newly identified states above 12.2 MeV since angular distribution measurements have yet to be performed. The state at 16.3 MeV is ~ 2 MeV higher than any previously known yrast state in a heavy nucleus.

The irregular transition energies indicate aligned-particle configurations along the yrast line up to the highest states observed. No evidence of collective excitations in the form of smoothly increasing transition energies has been discerned. This is also reflected in the fact that the decay times of the highest states are larger than ~2ps, the stopping time of the recoiling evaporation residues in the Pb backing of the target. The decay times have been inferred from the observation that the γ lines are sharp. The line shapes of transitions with decay times of $\lesssim$2 ps would show substantial Doppler broadening since the photon, detected at 0°, would be emitted from a slowing evaporation residue. On the other hand, such transitions would yield sharp lines which are Doppler shifted but not broadened if the residues were allowed to recoil into vacuum from thin targets. In an experiment with these conditions no extra lines were detected. Similar results have also been observed in ^{152}Dy [12].

The decay times have contributions from state lifetimes and feeding-times, which in principle can be separately determined from a recoil distance (plunger) measurement. If it turns out that the feeding

times are long, it would indicate single-particle structures at even higher spin and also above the yrast line. The number of non-discrete transitions preceding the highest state is small (6-10, assuming I_{max} = 55). Thus, a measurement of the feeding time will yield rather direct information on the character of the preceding cascade. It would also be of interest to determine if there is a connection between the feeding times and the slow statistical cascades which have been observed [13,14] in Er isotopes with A ~ 154.

In nuclei such as ^{147}Gd and ^{152}Dy the yrast lines reflect the oblate coupling scheme up to the highest observed spin. No evidence has so far been found for collective structures in discrete-line spectroscopy, although studies of the continuum cascades indicate collectivity above the yrast line [13-16]. It should also be kept in mind that the quadrupole moment of the $49/2^+$ isomer in ^{147}Gd implies $\beta \sim 0.2$ [17], a rather sizeable deformation which is also expected [18] for the higher states. Since no evidence has yet emerged for collective transitions in the immediate vicinity of the yrast line, the character of the collective excitations which are built on the very high spin aligned-particle configurations remains an interesting open problem.

Acknowledgements

One of the authors (D.F.) wishes to thank the Deutsche Forschungsgemeinschaft for financial support.

References

1. J. Pedersen, B. B. Back, F. M. Bernthal, S. Bjørnholm, J. Borggreen, O. Christensen, F. Folkmann, B. Herskind, T. L. Khoo, M. Neiman, F. Pühlhofer and G. Sletten, Phys. Rev. Lett. 39, 990 (1977).

2. R. Bengtsson, J. Y. Zhang and S. Åberg, Phys. Lett. 105B, 5 (1981).

3. A. Bohr and B. R. Mottelson, Physica Scripta 10A, 13 (1974).

4. B. Haas, D. Wand, H. R. Andrews, O. Häusser, A. J. Ferguson, J. F. Sharpey-Schafer, T. K. Alexander, W. Trautmann, D. Horn, P. Taras, P. Skensved, T. L. Khoo, R. K. Smither, I. Ahmad, C. N. Davids, W. Kutschera, S. Levenson and C. L. Dors, Nucl. Phys. A362, 254 (1981).

5. A. Pakkanen, Y. H. Chung, P. J. Daly, S. R. Faber, A. Helppi, J. Wilson, P. Chowdhury, T. L. Khoo, I. Ahmad, J. Borggreen, Z. W. Grabowski and D. C. Radford, Phys. Rev. Lett. 48, 1530 (1982).

6. H. Emling, E. Grosse, D. Schwalm, R. S. Simon and H. J. Wollersheim, Phys. Lett. 98B, 169 (1981); H. Emling, GSI Report No. GSI-82-40 (to be published).

7. D. Ward, H. R. Andrews, O. Häusser, Y. El Masri, M. M. Aléonavd, I. Yang-Lee, R. M. Diamond, F. S. Stephens and P. A. Butler, Nucl. Phys. A332, 433 (1979).

8. R. J. Liotto and R. Sorensen, Nucl. Phys. A297, 136 (1978).

9. T. Byrski, F. A. Beck, C. Gehringer, J. C. Merdinger, Y. Schutz, J. P. Vivien, J. Dudek, W. Nazarewicz and Z. Szymánski, Phys. Lett. 102B 235 (1981).

10. C. G. Anderson, R. Bengtsson, T. Bengtsson, J. Krumlinde, G. Leander, K. Neergaard, P. Olanders, J. A. Pinston, J. Ragnarsson, Z. Szymański and S. Åberg, Physica Scripta 24, 266 (1981).

11. O. Bakkander, C. Baktash, J. Borggreen, J. E. Jensen, J. Kownacki, J. Pedersen, G. Sletten, D. Ward, H. R. Andrews, O. Häusser, P. Skensved and P. Taras, Nucl. Phys. A, in press.

12. K. Broda, P. Kleinheinz, S. Lunardi, J. Styczen and J. Blomqvist, Z. Phys. A305, 281 (1982).

13. A. Hübel, R. M. Diamond, P. Aguer, C. Ellegaard, D. B. Fosson, H. Kluge, C. Schück, S. Shih, F. S. Stephens and U. Smilanski, Z. Phys. A304, 225 (1982).

14. P. Chowdhury, et al., to be published.

15. P. Chowdhury, J. Borggreen, T. L. Khoo, I. Ahmad, R. K. Smither, S. R. Faber, P. J. Daly, C. L. Dors and J. Wilson, Phys. Rev. Lett. 47, 778 (1981).

16. N. Rud, D. Ward, H. R. Andrews, P. Taras, J. Keinonen, Phys. Lett. 100B, 17 (1981).

17. O. Häusser, H.-E. Mahnke, J. F. Sharpey-Schafer, M. L. Swanson, P. Taras, D. Ward, H. R. Andrews and T. K. Alexander, Phys. Rev. Lett. 44, 132 (1980).

18. T. Døssing, K. Neergaard and H. Sagawa, Physica Scripta 24, 258 (1981).

Figure Captions

Fig. 1. Modes of generating angular momentum as a function of neutron number and spin.

Fig. 2. Level scheme of ^{154}Dy.

Fig. 3. Plot of I_x vs $\hbar\omega$ for ^{154}Dy. Dashed lines connect different yrast structures.

Fig. 4. Spin dependence of Q_0(eff), defined as $[B(E2\ I \to I-2)\ 16\pi/5]^{1/2} / \langle I\ 2\ 0\ 0 \mid I-2\ 0 \rangle$. For $I > 10$ the Clebsch-Gordon coefficient is almost constant and the right hand ordinate shows approximate B(E2) - values in Weisskopt units.

Fig. 5. Schematic representation of the transition from prolate to triaxial to oblate shapes, which probably occurs in ^{154}Dy.

Fig. 6. Schematic representation of the motion of high-j particle orbits in the strong coupling and decoupling limits. The top part shows the precession of the particle spin vector about the symmetric and perpendicular axes. The bottom part shows the particle orbits viewed along the perpendicular (rotation) axis. In the decoupling limit the precession around the perpendicular axis leads to an oblate mass distribution with respect to this axis for the orbit.

Fig. 7. (a) Rotational frequency fluctuation of the surface of a neutron star. (b) Rotational frequency of the nuclear core as a function of time t following the ^{124}Sn (^{34}S, 4n)^{154}Dy reaction at 155 MeV. Abrupt changes correspond either to

the departure from oblate shapes or to backbends.

(c) Aligned particle spin, i, as a function of t. Changes in i give rise to corresponding fluctuations in the core frequency shown in (b).

Fig. 8. 'Phases' of even Dy nuclei as a function of spin and neutron number. The different modes of generating yrast spin are indicated. The hashes indicate the limits of present experimental knowledge. The theoretical prediction of Ref. 2 and 10 are also indicated.

Fig. 9. Preliminary level scheme of ^{147}Gd.

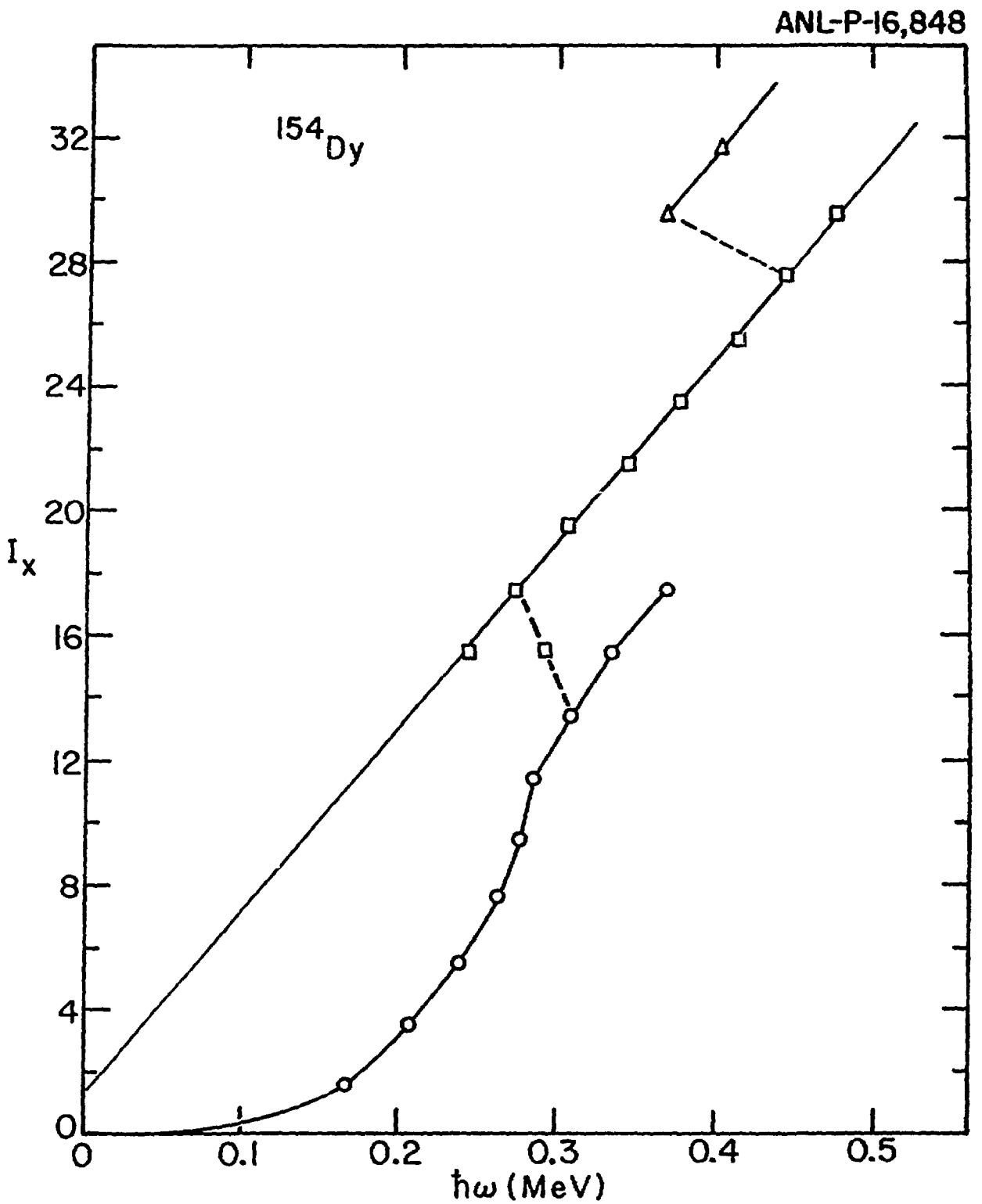

Fig. 3

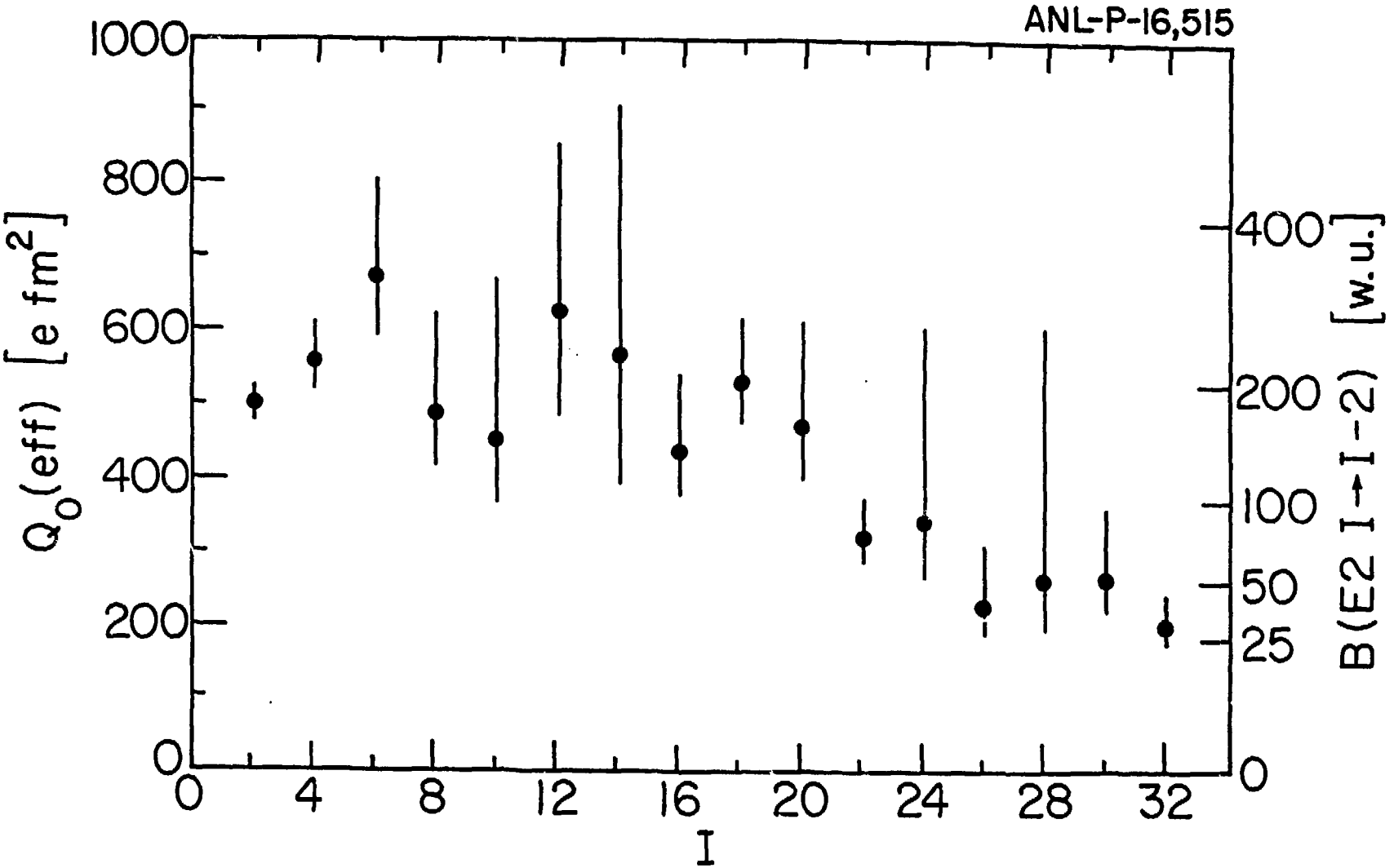
ANL-P-16,515
1000
800
600
400
200
0
Q_0(eff) [e fm^2]
400
200
100
50
25
0
B(E2 I→I-2) [w.u.]
0
4
8
12
16
20
24
28
32
I

Fig. 4

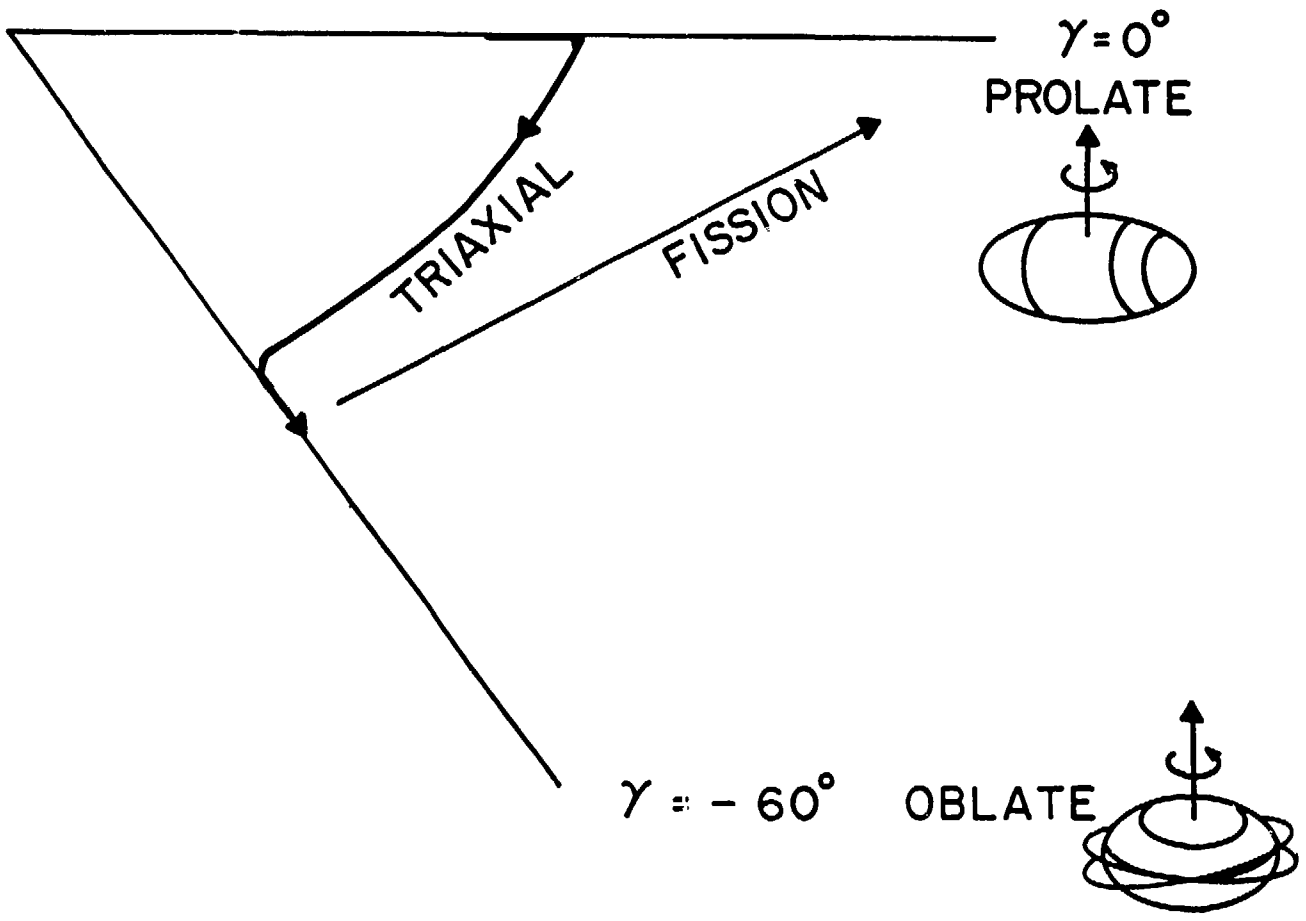

Fig. 5

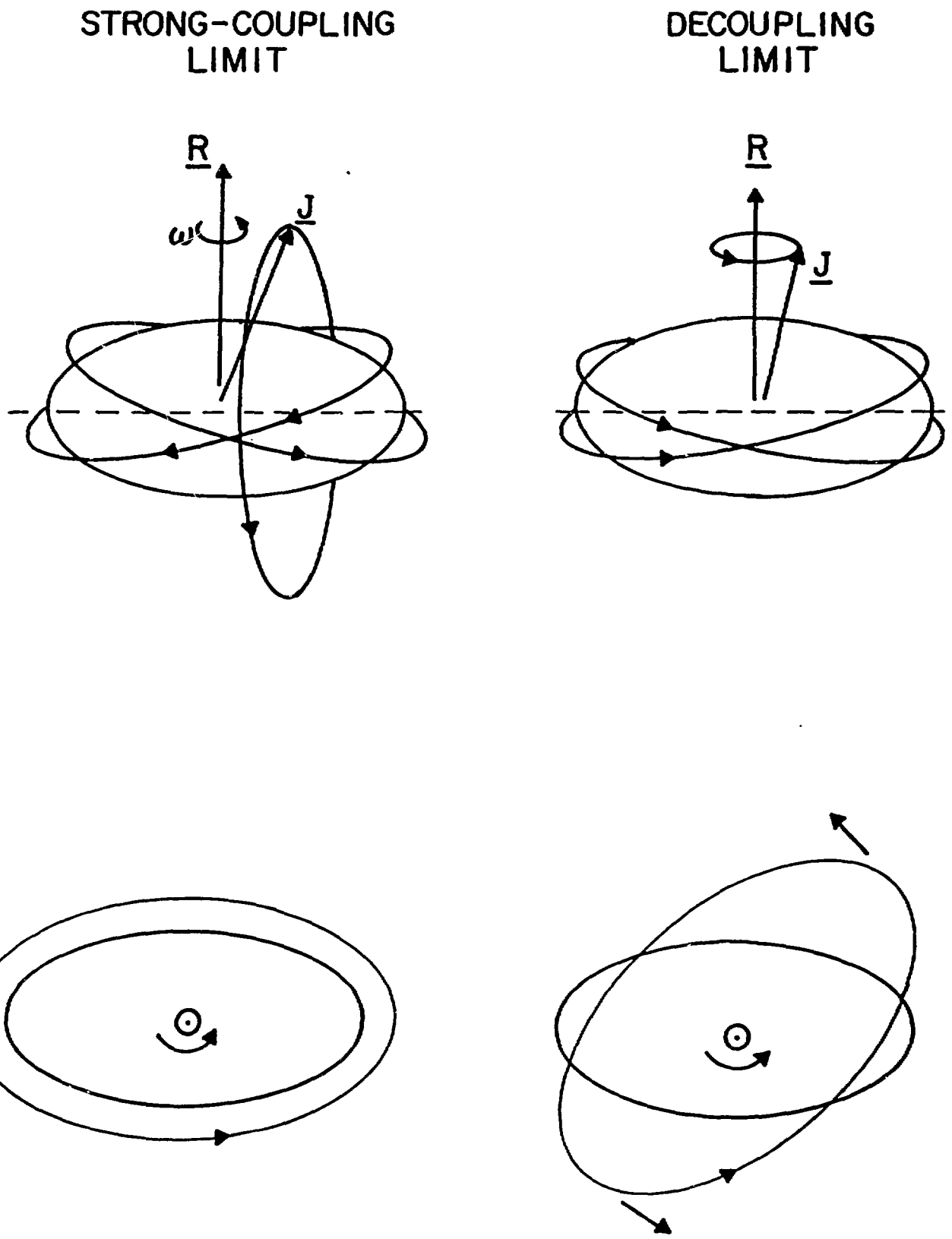

Fig. 6

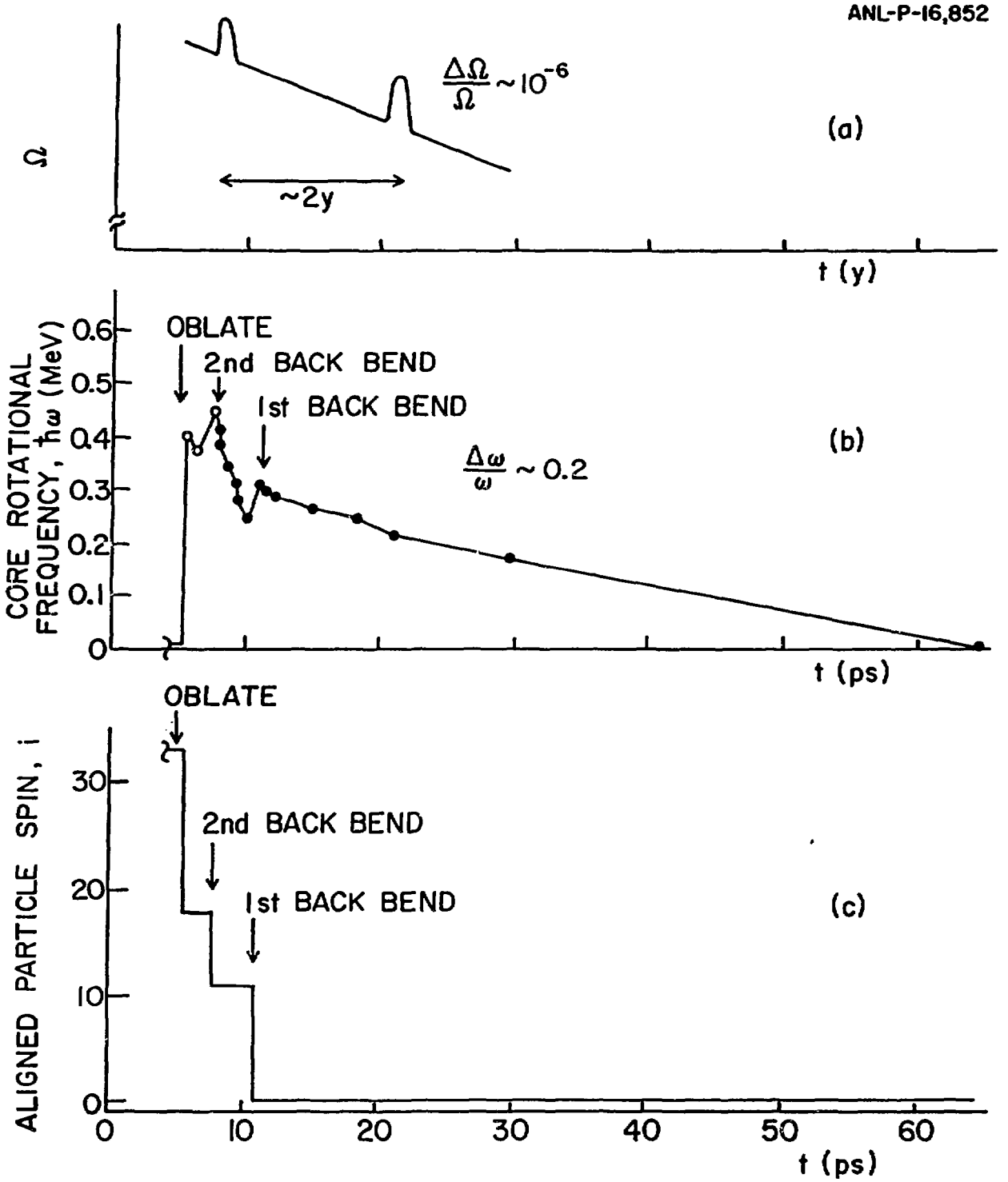
ANL-P-16,852
Ω
$\frac{\Delta\Omega}{\Omega} \sim 10^{-6}$
~2y
(a)
t (y)
CORE ROTATIONAL FREQUENCY, ħω (MeV)
0.6
0.5
0.4
0.3
0.2
0.1
0
OBLATE
2nd BACK BEND
1st BACK BEND
$\frac{\Delta\omega}{\omega} \sim 0.2$
(b)
t (ps)
OBLATE
ALIGNED PARTICLE SPIN, i
30
20
10
0
2nd BACK BEND
1st BACK BEND
(c)
0
10
20
30
40
50
60
t (ps)

Fig. 7

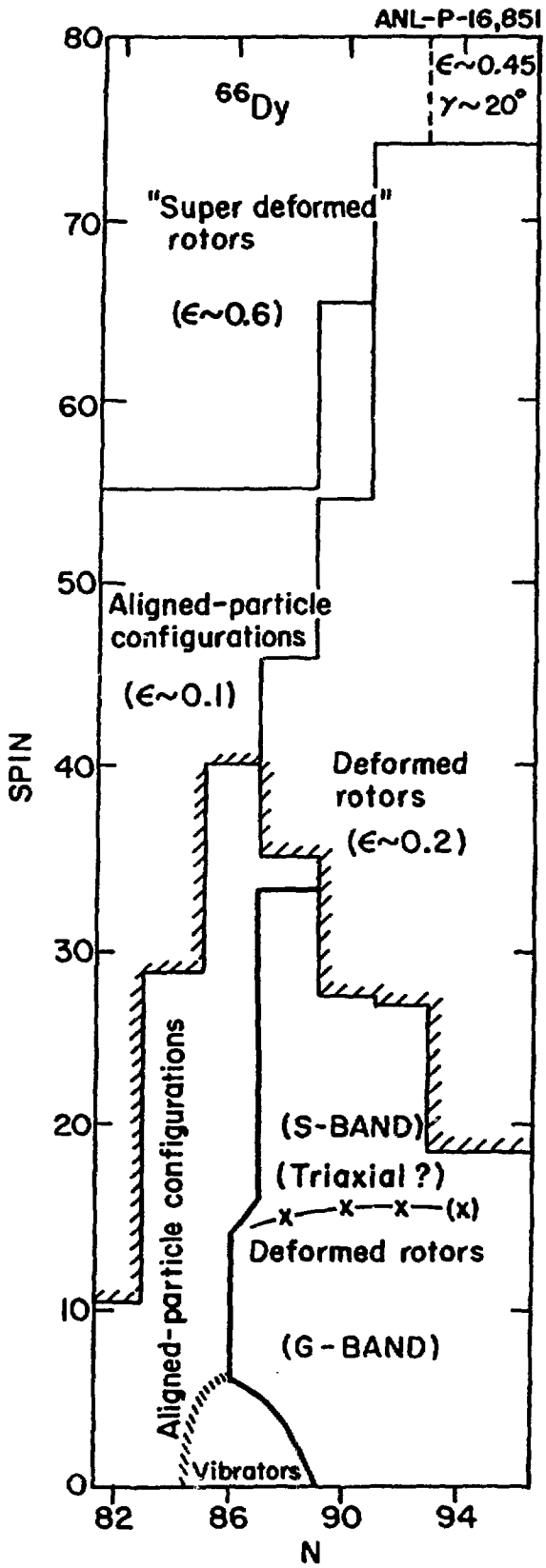
ANL-P-16,851
80
70
60
50
40
30
20
10
0
SPIN
82
86
90
94
N
^{66}Dy
ϵ~0.45
γ~20°
"Super deformed" rotors
(ϵ~0.6)
Aligned-particle configurations
(ϵ~0.1)
Deformed rotors
(ϵ~0.2)
(S-BAND)
(Triaxial ?)
x—x—x—(x)
Deformed rotors
(G-BAND)
Aligned-particle configurations
Vibrators

Fig. 8

Fig. 9 to be prepared in Denmark

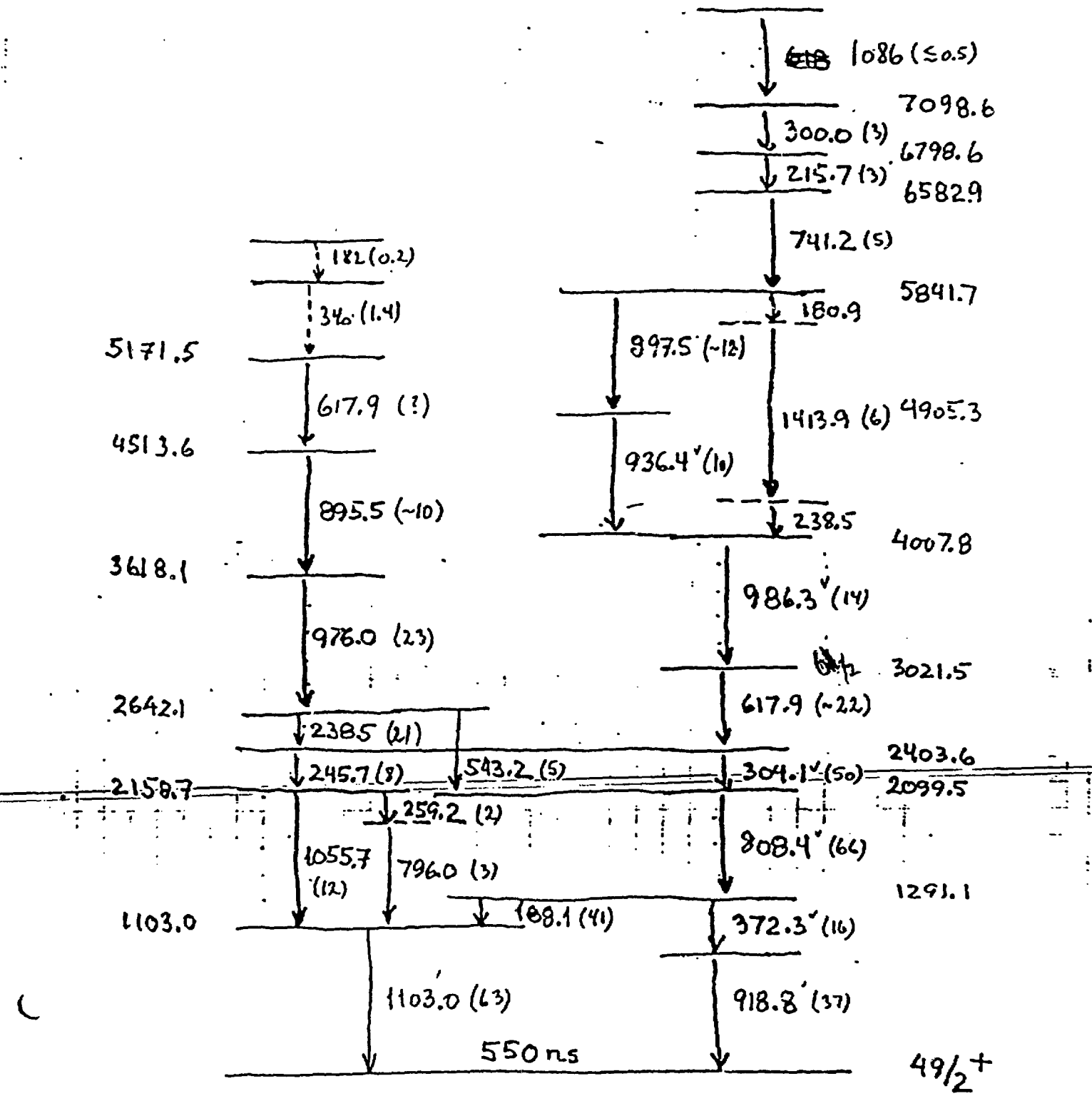

DISCLAIMER